January 2004

Measurement of Electrode Overpotentials for Direct Hydrocarbon Conversion Fuel Cells

Venkatesan V. Krishnan
University of Pennsylvania

Steven McIntosh
University of Pennsylvania

Raymond J. Gorte
University of Pennsylvania, gorte@seas.upenn.edu

John M. Vohs
University of Pennsylvania, vohs@seas.upenn.edu

Follow this and additional works at: http://repository.upenn.edu/cbe_papers

Measurement of Electrode Overpotentials for Direct Hydrocarbon Conversion Fuel Cells

Abstract

Cathodic and anodic overpotentials were measured using current interruption and AC impedance spectroscopy for two separate solid oxide fuel cells (SOFCs). The fuel cells used yttria-stabilized zirconia (YSZ) as the electrolyte, strontium-doped lanthanum manganite (LSM) as the cathode, and a porous YSZ layer impregnated with copper and ceria as the anode. The $Cu/CeO_2/YSZ$ anode is active for the direct conversion of hydrocarbon fuels. Overpotentials measured using both current interruption and impedance spectroscopy for the fuel cell operating at 700ºC on both hydrogen and n-butane fuels are reported. In addition to providing the first electrode overpotential measurements for direct conversion fuel cells with Cu-based anodes the results demonstrate that there may be significant uncertainties in measurements of electrode overpotentials for systems where there is a large difference between the characteristic frequencies of the anode and cathode processes and/or complex electrode kinetics.

Comments

Measurement of Electrode Overpotentials for Direct Hydrocarbon Conversion Fuel Cells

Venkatesan V. Krishnan, Steven McIntosh,
Raymond J. Gorte, and John M. Vohs[*]

Department of Chemical and Biomolecular Engineering,
University of Pennsylvania,
Philadelphia, PA 19104.

ABSTRACT

Cathodic and anodic overpotentials were measured using current interruption and AC impedance spectroscopy for two separate solid oxide fuel cells (SOFCs). The fuel cells used yttria-stabilized zirconia (YSZ) as the electrolyte, strontium-doped lanthanum manganite (LSM) as the cathode, and a porous YSZ layer impregnated with copper and ceria as the anode. The $Cu/CeO_2/YSZ$ anode is active for the direct conversion of hydrocarbon fuels. Overpotentials measured using both current interruption and impedance spectroscopy for the fuel cell operating at 700°C on both hydrogen and n-butane fuels are reported. In addition to providing the first electrode overpotential measurements for direct conversion fuel cells with Cu-based anodes the results demonstrate that there may be significant uncertainties in measurements of electrode overpotentials for systems where there is a large difference between the characteristic frequencies of the anode and cathode processes and/or complex electrode kinetics.

[*] corresponding author

INTRODUCTION

Cu-ceria-YSZ cermet anodes for solid oxide fuel cells (SOFCs) developed by Gorte and co-workers [1-5] have been shown to be active for the direct conversion of hydrocarbon fuels at temperatures below 800°C. Unlike the more commonly used Ni-YSZ cermet anodes, Cu-ceria-YSZ cermets do not catalyze the formation of carbon deposits from hydrocarbons and, therefore, do not require that the fuel be reformed into a hydrogen rich synthesis gas. The overall performance (I-V curves) for cells with Cu-ceria-YSZ anodes while operating on a variety of hydrocarbon fuels, including butane, decane and toluene, has been reported in numerous previous investigations [1-6]. In order to improve the performance of SOFCs that are designed to operate directly on hydrocarbon fuels, the overpotentials and area specific resistances (ASR) of the individual cell components, especially the Cu-ceria-YSZ cermet anode, need to be accurately measured as a function of cell current. In this study we report the first such measurements on cells with a Cu-ceria-YSZ anode, YSZ electrolyte, and LSM-YSZ cathode.

Two methods are commonly used to measure overpotentials of the electrodes in a SOFC: AC impedance spectroscopy and current interruption. Descriptions of the experimental set-ups for these techniques and the methods of data analysis are well documented in the literature [6-8]. In impedance spectroscopy one measures the transient response of a cell when subjected to a sinusoidal voltage of low amplitude. This technique is often used to measure overpotentials using symmetric half-cells (e.g. cathode/electrolyte/cathode). While this approach may be generally applicable for cathodes, for anodes it can only be used to measure overpotentials near open circuit. Since the area specific resistance (ASR) of direct oxidation anodes vary significantly with current density this approach is not of great utility for these anodes. Anode overpotentials as a function of current density can be measured using impedance spectroscopy, however, if a test cell with a well placed reference electrode is employed. The overpotential of each electrode, η is related to the resistance according to $R_p = d\eta/dj$ (j being the current density) and calculated by integration of the measured electrode resistance from zero current to the current of interest. The need to integrate the ASR values over a range of currents can result in some uncertainty in the measurement of

electrode overpotentials using this technique. This is especially true for direct oxidation fuel cells where, as noted above, the ASR of the anode varies significantly with current.

Current interruption provides a more direct method to measure electrode overpotentials. In this technique the transient response of the voltage of the electrode relative to a reference electrode is measured following interruption of the cell current. Since the electrolyte is essentially Ohmic, the voltage drop associated with the electrolyte occurs nearly instantaneously following current interruption. The overpotential, η_A, of the anode in a current interruption measurement is given by $\eta_A = OCV - V_{IR,A}$, where OCV is the open circuit voltage and, $V_{IR,A}$, is the voltage between the anode and the reference electrode immediately following current interruption. The overpotential of the cathode, η_C, is given by the voltage difference between the cathode and the reference electrode, $V_{IR,C}$, immediately following current interruption.

In order to completely separate the anode and cathode processes a well-placed reference electrode is again required. Several recent experimental and theoretical studies have demonstrated the importance of well-designed cell geometry in order to obtain a reference electrode whose potential is pinned near the center of the electrolyte and independent of cell current [9-13]. These studies show that one needs to use a cell with a relatively thick electrolyte, symmetric coaxial placement of the cathode and anode, and placement of the reference electrode at least three electrolyte thicknesses from the edge of one of the electrodes. Alternate pellet geometries have also been suggested in which the reference electrode is physically imbedded in the center of an electrolyte layer that is several millimeters in thickness [12, 13].

The criteria for well-designed three electrode cells are rather stringent and can be difficult to adhere to. This is especially true for SOFCs that directly utilize hydrocarbons fuels. For higher hydrocarbons such as butane, gas phase reactions that result in tar formation and carbon deposition on the anode become significant at temperatures greater than ~750°C. Sintering of the Cu layer that is used as the current collector in the anode is also a problem for temperatures greater than 800°C. Thus, direct oxidation SOFCs with Cu/CeO$_2$ anodes must be operated at temperatures less than ~750°C. Due to the low ionic conductivity of the YSZ electrolyte in this temperature range relatively large voltages are required in this temperature range for a cell with a thick electrolyte in order

to obtain reasonable current densities. The high ASR of a thick electrolyte layer may also result in significant IR heating of the cell during data collection at high current densities. This would be particularly problematic in test cells with electrolyte layers several millimeters in thickness and may cause significant temperature drift. All of these factors make it more difficult to use test cell geometries with thick electrolyte layers when working with direct oxidation cells.

At least in the case of impedance spectroscopy it has been shown that even when using a test cell geometry that adheres to the criteria given above, significant errors in the measurement of ASRs and overpotentials due to cross talk between the anode and cathode may arise if there is a large difference between the characteristic frequencies of the cathodic and anodic processes [13]. This phenomenon manifests itself as inductance loops or extra lobes in the cathode or anode impedance spectra that are centered at the characteristic frequency of the other electrode. A detailed analysis of these anomalous effects arising in the AC impedance spectra for direct oxidation fuel cells with Cu-ceria-YSZ cermet anodes has recently been presented by McIntosh et al [6]. In theory, this cross talk phenomenon should also manifest itself in current interruption measurements of electrode overpotentials. The influence of cross talk on current interruption measurements has yet to be evaluated experimentally, however.

In this paper we report the first current interruption measurements of cathode and anode overpotentials for direct conversion SOFCs with Cu-ceria-YSZ anodes, YSZ electrolyte, and LSM-YSZ cathodes. Impedance spectroscopy overpotential measurements are also presented and used for comparison purposes and to assess the quality of our test cell configuration. The influence of cell geometry on the accuracy of current interruption measurements was further investigated and the presence of cross talk between the anode and cathode in a current interruption measurement was demonstrated for the first time. How this latter effect influences the accuracy of the overpotential measurements is also discussed.

EXPERIMENTAL

YSZ electrolyte supported solid oxide fuel cells with $Cu/CeO_2/YSZ$ and LSM/YSZ composite anodes and cathodes, respectively, were used in this study. The

methods used to synthesize the ceramic components in these fuel cells have previously been described in detail [1, 2]. Briefly, the cells were constructed by initially laminating a green semi-circular YSZ tape containing graphite pore formers onto a circular green YSZ electrolyte tape. This bi-layer was then calcined in air at 1550°C for 4 hours producing a porous 300 μm thick YSZ layer supported on a dense 750 μm thick YSZ electrolyte disc approximately 11 mm in diameter. After forming the anode, the cathode was applied to the opposite side of the cell by applying a paste containing 50% wt lanthanum strontium manganate (LSM) and 50% wt YSZ in glycerol [1, 2]. Care was taken to ensure that the cathode had the same semicircular shape as the anode and was spatially aligned with the anode. A small spot of the LSM-YSZ paste was painted near the edge of the electrolyte disc and used as a reference electrode. The area of the electrodes was 0.48 cm^2. Figure 1(a) shows a schematic of the configuration of this cell.

The second cell used in this study had a slightly different geometry (see Figure 1(b)) and the anode was made using poly-methyl methacrylate (PMMA) and graphite as the pore-formers [1, 2]. The anode and cathode in this cell were circular with exactly the same dimensions and placed co-axially with the electrolyte. The reference electrode was painted as a spot of LSM-YSZ paste, near the edge of the electrolyte. The procedure for making the cell is described in detail by McIntosh et al. [6]. The thickness of the electrolyte layer in this cell was 360 μm and that of the porous layer was 600 μm, after calcination. The area of each electrode was 0.28 cm^2.

For both cells, after painting on the cathodes, the cell was calcined at 1250°C for 2 hours. The anode was then impregnated with ceria (10% by weight) and then copper (20% by weight) in the following manner. The anode was first saturated with an aqueous solution of $Ce(NO_3)_3$ and then calcined for 30 min at 450°C. This step was repeated several times in order to obtain a 10% by weight loading of ceria. As similar procedure employing an aqueous solution of $Cu(NO_3)_2$ was then used to add Cu to the anode. Reduction of the CuO formed after calcination was accomplished by exposing the cell to hydrogen when it was first heated to the operating temperature of 700°C.

During fuel cell testing the cathode was exposed to air and fuel (H_2 or n-C_4H_{10}) was administered to the anode. All measurements were made at cell temperature of 700°C. As described previously, in order to obtain good performance with H_2, the anode

had to be initially conditioned by exposing it to n-C_4H_{10} for several minutes at 700°C [6]. The primary reaction products during operation on n-C_4H_{10} were CO_2 and H_2O.

Current interruption measurements were carried out using a transistor as a fast solid-state switch. Data was collected using a digital storage oscilloscope (Tektronix TDS 3032B). For cell voltages between OCV and zero the current was varied by adjusting the resistance of the external load. In order to obtain data at higher current densities an external voltage was applied to the cell using a Tektronix PS 280 power supply. AC Impedance spectra of the cathode and the anode were obtained relative to the reference electrode in the galvanostatic mode, using a Gamry Instruments Model EIS 300 impedance spectrometer. Measurements were made for frequencies ranging from 0.01 to 100,000 Hz with the AC rms amplitude of 0.001 A. Impedance spectra were also measured across the entire cell (i.e. anode to cathode) in order to determine the overall cell impedance and Ohmic resistance.

RESULTS and DISCUSSION

The I-V characteristics for the cells used in this study while operating on hydrogen and n-butane fuels are at 700°C are displayed in Figures 2(a) and 2(b). The I-V curves for H_2 are nearly linear indicating constant area specific resistances (ASRs) for the anode and cathode. In contrast for n-C_4H_{10} the I-V curves are highly non-linear at low current densities. This behavior is consistent with what has been reported previously for direct oxidation SOFCs of a similar design [1, 2, 4, and 6] and is indicative of complex kinetics for the anode process.

The current interruption technique was used to measure the cathode and anode overpotentials for both cells. For cell 1, the ASR of the electrolyte was determined to be 2.95 Ohm-cm^2 in hydrogen and 2.90 Ohm-cm^2 in n-butane by the current interruption and AC impedance methods. Cell 2 was identical to the one used in the study of McIntosh et al. [6] and since the electrodes were circular in shape, it was more symmetric than cell 1. The ASR of the electrolyte for this cell was found to be 2.55 Ohm-cm^2 in hydrogen and 2.45 Ohm-cm^2 in n-butane using the both current interruption and impedance spectroscopy.

As has been discussed in detail in several previous studies, proper alignment of the cathode and anode and positioning of the reference electrode are required in order to obtain accurate measurements of overpotentials using both current interruption and impedance spectroscopy [9-13]. For a cell with an ideal configuration the magnitude of the initial drop in the reference to cathode current interruption measurement should be equal to that in the reference to anode measurement at the same current density. This criterion assumes that that the initial, abrupt drop following current interruption is due primarily to the Ohmic resistance of the electrolyte. The electrolyte conductivity obtained from the Ohmic resistances determined using current interruption were 0.025 S/cm (cell 1) and 0.015 S/cm (cell 2). These values are within the range of ionic conductivities for YSZ of 0.01 to 0.02 S/cm [14], which are reported in the literature. Therefore, the assumption that the resistances of the electrodes do not contribute significantly to the initial drop following current interruption appears to be justified. The split in the Ohmic resistance between the cathode and reference electrode and the anode and reference electrode for cell 1 was approximately 80-20 %. The split in the electrolyte Ohmic resistance between cathode to reference and anode to reference for cell No. 2 was 60-40 %. This suggests that cell 2 was closer to the ideal geometry.

The overpotentials of the anode and the cathode for cell 1 determined using current interruption as a function of current density are plotted in Figures 3(a) and 3(b), respectively. The plot of the anodic overpotential versus current density for n-C_4H_{10} is non-linear indicating that for this fuel the anode ASR is a function of the current density. This result is consistent with the non-linear I-V curve for this cell while operating on n-C_4H_{10}. Since the cathodic process does not depend on the fuel exposed to the anode, the differences in the I-V curves for hydrogen and n-butane fuels should be accounted for solely by changes in the overpotential of the anode. The data are not consistent with this conclusion, however. Note that for current densities greater than 0.2 A/cm^2 the difference in the anode overpotential for butane and hydrogen fuels is relatively constant at ~200 mV, while the difference in the I-V curves for these two fuels is roughly 280 mV. As shown in Figure 3(b) the measured overpotential of the cathode also changes significantly as the fuel exposed to the anode is switched from hydrogen to n-butane.

These results further demonstrate that the geometry of cell 1 does not lend itself to accurate measurement of electrode overpotentials.

Plots of the anode and cathode overpotentials measured using current interruption as a function of cell current density for cell 2 for both H_2 and n-C_4H_{10} fuels are displayed in Figure 4(a) and 4(b), respectively. Many of the features of these plots are similar to those obtained for cell 1. In particular, the plot of the anode overpotential for H_2 is linear while that for n-C_4H_{10} is highly non-linear, especially at low current densities.

While the measured anode overpotentials are similar for both cells, there are large differences in the measured cathode overpotentials. As shown in Figure 4(b), for cell 2 the cathode overpotentials are significantly less than those measured for cell 1 despite the fact that both cells have cathodes that were constructed in the same manner. Although there is some spread in the data for cell 2, as would be expected, there is relatively little variation in the cathode overpotential as the fuel exposed to the anode was switched from hydrogen to n-butane. The difference in the anode overpotential as the fuel was switched is also consistent with the I-V curves for cell 2. For example, at current densities between 0.05 and 0.1 A/cm^2 the difference in the cell voltage for H_2 and n-C_4H_{10} fuels is roughly 300 mV (see Figure 2(b)). In this current range the difference between the hydrogen and n-butane anodic overpotential is varies between 300 and 330 mV (see Figure 4(a)). These results further confirm that the geometry of cell 2 is much better than that of cell 1 for these types of measurements. Thus, the overpotentials determined by the current interruption technique, especially those for the cathode, are more accurate for cell 2 that those for cell 1.

Although the current interruption data for cell 2 appear to satisfy all of the internal consistency checks (i.e. reasonable Ohmic split between the anode and cathode relative to the reference electrode and the cathode overpotential is independent of the fuel exposed to the anode), there are still potential sources of error in the overpotential measurements. As noted in the introduction, even for a cell with an ideal geometry cross talk between the electrodes can occur if there is a large difference in the characteristic anode and cathode frequencies. We have previously used impedance spectroscopy to characterize the anode and cathode in cells similar to those used in the present study [6]. In this previous study it was found that for operation in H_2 the characteristic frequencies of the anodic and

cathodic processes were 4 Hz and 2 kHz, respectively. Thus, cross talk may occur for these cells. The impedance spectra for cell 2 presented in Figure 5 demonstrates that this is indeed the case. This figure displays impedance spectra for the anode and cathode relative to the reference electrode at a current density of 0.2 A/cm^2 for both hydrogen and n-butane fuels. The impedance spectrum for the entire cell measured anode to cathode is also presented in the figure. These spectra are consistent with those reported in our previous study and show that the anode and cathode spectra are dominated by lobes centered at 4 Hz and 2 kHz, respectively [6]. Note, however, that the spectrum for the cathode while running on H$_2$ contains a smaller well-resolved lobe centered at the primary frequency of the anode. While not as well resolved a similar lobe is apparent in the cathode spectrum for n-butane. An inductance artifact is also present in the cathode spectrum while operating with n-butane. As described in detail by McIntosh et al. [6] and Adler [13] both of these effects can be attributed cross talk between the two electrodes.

Since impedance spectroscopy and current interruption are complimentary frequency and time space characterization methods, one would expect the cross talk phenomenon to manifest itself in the data from both techniques. This is indeed the case. Figure 6 displays a portion of a cathode transient voltage decay signal following current interruption for cell 2 operating on H$_2$ at a current density of 0.1 A/cm^2. Two curve fits to this data are also presented in the figure. Equation 1 is the best fit using a single exponential function with a characteristic cathodic frequency of 2 kHz, which was determined via impedance spectroscopy. Note that this equation fits the data very well for the first 250 μs. At longer times, however, the single exponential decay significantly underestimates the experimental data. Equation 2 is the best fit obtained using a sum of two exponential decays. One of the exponential terms again uses the characteristic cathodic frequency of 2 kHz, while the other uses the characteristic anodic frequency of 4 Hz. This latter term represents the cross talk between the cathode and anode that was observed in the impedance spectroscopy measurements. Note that this equation provides a better fit to the data, especially at longer times. Thus as expected, cross talk is also present in the current-interruption data.

Unfortunately, it is difficult to quantify how much error is introduced into the current interruption measurements of the overpotentials by cross talk between the anode and cathode. For the cells used in this study the overpotential of the anode was significantly larger than that of the cathode. Thus, cross talk is likely to introduce relatively small errors in the anode overpotential measurements. The effect would be more significant, however, for the cathode overpotentials. The cathode impedance spectrum in Figure 5 shows that the width of the cross-talk lobe centered at 4 Hz is roughly 30 % of that of the primary lobe centered at 2 kHz. This suggests that the cathode overpotentials may be overestimated by almost 30 %.

For comparison purposes, cathode and anode overpotentials were also estimated by integration of electrode resistances determined from impedance spectra. Table 1 lists the overpotentials as a function of current density measured by both techniques for both H_2 and n-C_4H_{10} fuels. The values of the overpotentials obtained by both methods are similar for current densities less than 0.1 A/cm^2. At higher current densities there is a marked difference in the anode overpotentials for n-butane measured by the two methods with the current interruption technique consistently giving lower values. As discussed earlier, these differences are most likely due to higher uncertainties associated with the impedance spectroscopy technique compared to current interruption, for systems with non-linear kinetics.

CONCLUSIONS

Current interruption and AC impedance methods were used for the first time to measure overpotentials for Cu-CeO$_2$-YSZ anodes and LSM-YSZ cathodes in direct oxidation fuel cells while operating on both H_2 and n-C_4H_{10} fuels. The influence of experimental errors arising due to the test cell geometry and cross talk between the anode and cathode on the accuracy of the overpotential measurements was assessed. The presence of cross talk between the anode and cathode in current interruption measurements was also experimentally verified.

In addition to providing the first measurements of electrode overpotentials for direct oxidation fuel cells with Cu-based anodes, this study serves to further demonstrate that there may be significant uncertainties in measurements of electrode overpotentials

for systems where there is a large difference between the characteristic frequencies of the anode and cathode processes and/or complex electrode kinetics.

ACKNOWLEDGMENTS

REFERENCES

1. R. J. Gorte, S. Park, J. M. Vohs, and C. Wang, *Adv. Mater.*, **12** (2000) 1465.

2. S. Park, R. J. Gorte, and J. M. Vohs, *J. Electrochem. Soc.*, **148(5)** (2001) A443.

3. H. Kim, J. M. Vohs, and R. J. Gorte, *Chem. Commun.*, **Issue 22** (2001) 2334.

4. S. Park, J. M. Vohs, and R. J. Gorte, *Nature*, **404** (2000), p. 265.

5. H. Kim, S. Park, J. M. Vohs, and R. J. Gorte, *J. Electrochem. Soc.*, **148(7)** (2001) A693.

6. S. McIntosh, J. M. Vohs, and R. J. Gorte, *J. Electrochem. Soc.*, submitted.

7. S. P. S. Badwal and N. Nardella, *Solid State Ionics*, **40/41** (1990) 878.

8. N. Nardella, D. V. Ho, and S. P. S. Badwal, *Mater. Sci. Forum*, **34-36** (1988) 237.

9. M. Nagata, Y. Itoh, and H. Iwahara, *Solid State Ionics*, **67** (1994) 215.

10. F. M. Figueiredo, J. Frade, and F. M. B. Marques, *Bol. Soc. Esp. Ceram. Vidrio*, **38(6)** (1999) 639.

11. S. H. Chan, X. J. Chen, and K. A. Khor, *J. App. Electrochem.*, **31** (2001) 1163

12. J. Winkler, P. V. Hendriksen, N. Bonanos, and M. Mogensen, *J. Electrochem. Soc.,* **145(4)** (1998) 1184.

13. S. B. Adler, *J. Electrochem. Soc.*, **149(5)** (2002) E166.

14. *Fuel Cell Handbook, 6th Edition*, EG&G Technical Services, Inc., Chapter 7, Page 4.

Table 1. **Comparison of Overpotentials obtained by Current Interruption (CI) and by AC Impedance (ACI) Spectroscopy (values are in Volts)**

Fuel	Electrode	I, A/cm^2 Technique	0.025	0.05	0.075	0.10	0.20	0.30
Hydrogen	Cathode	CI	-	0.05	-	0.11	0.14	0.15
"	"	ACI	-	-	-	0.08	0.15	0.20
"	Anode	CI	-	0.06	-	0.10	0.18	0.25
"	"	ACI	-	-	-	0.07	0.15	0.24
n-Butane	Cathode	CI	-	0.056	0.06	0.06	0.11	0.15

FIGURE CAPTIONS

Figure 1.   Schematic diagrams of (a) cell 1 and (b) cell 2.

Figure 2.   I-V curves for hydrogen and n-butane fuels at 700°C for (a) cell 1 and (b) cell 2.

Figure 3.   (a) Anode and (b) cathode overpotentials for cell 1 operating on hydrogen and n-butane at 700°C.

Figure 4   (a) Anode and (b) cathode overpotentials for cell 2 operating on hydrogen and n-butane at 700°C.

Figure 5:   Impedance spectra obtained from cell 2 with hydrogen (lower panel) and n-butane (upper panel) fuels at 0.2 A/cm^2 and 700°C.

Figure 6:   Current versus time following current interruption for cell 2 operating on H$_2$ at 0.1 A/cm^2 and 700°C. The curve fits are described in the text.
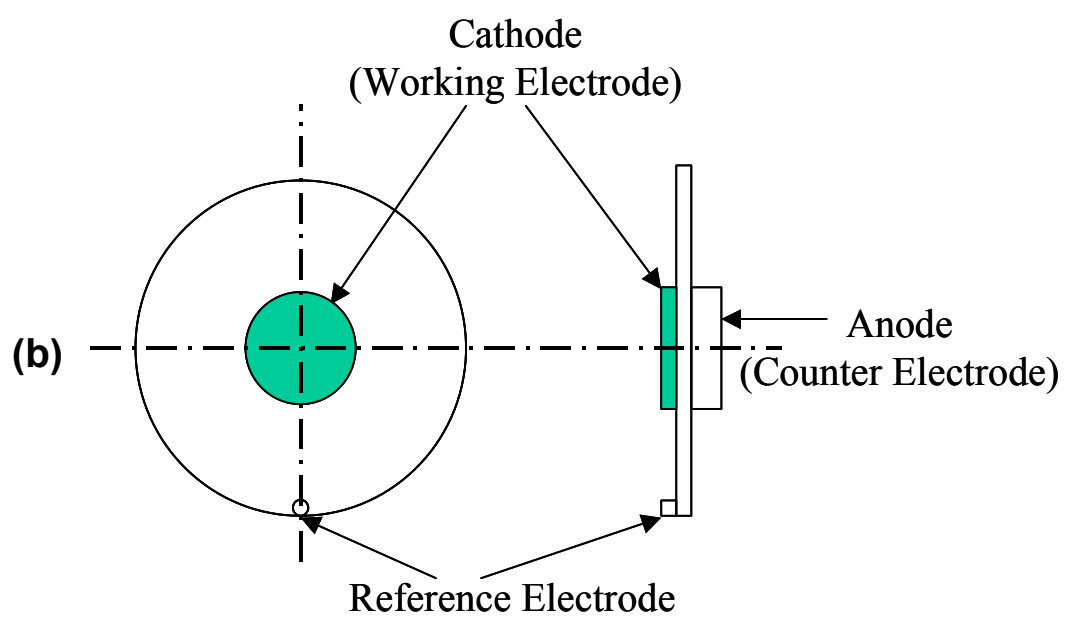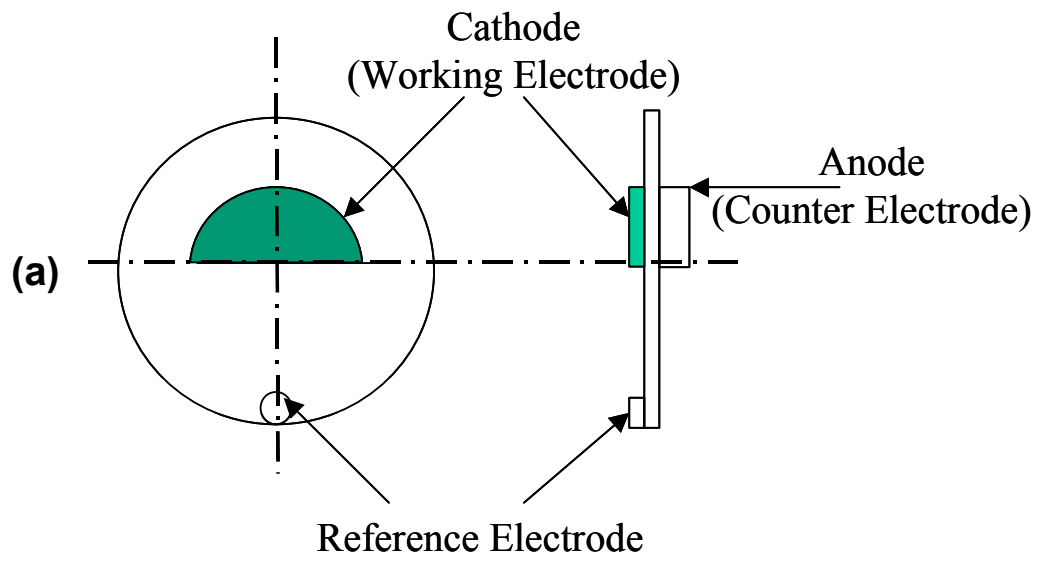
Figure 1
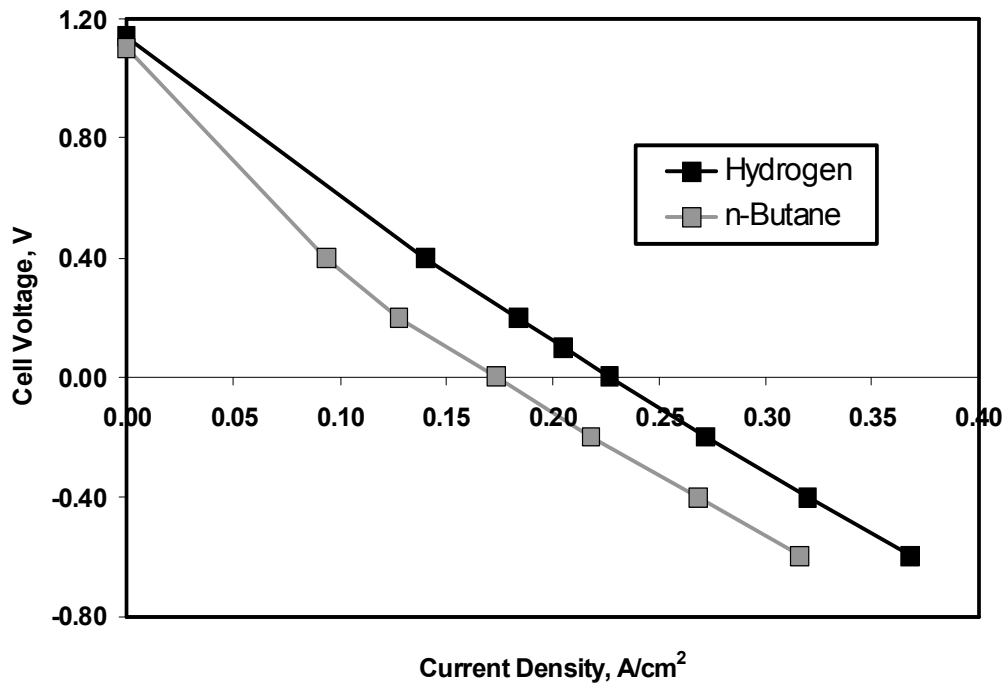
Figure 2(a)
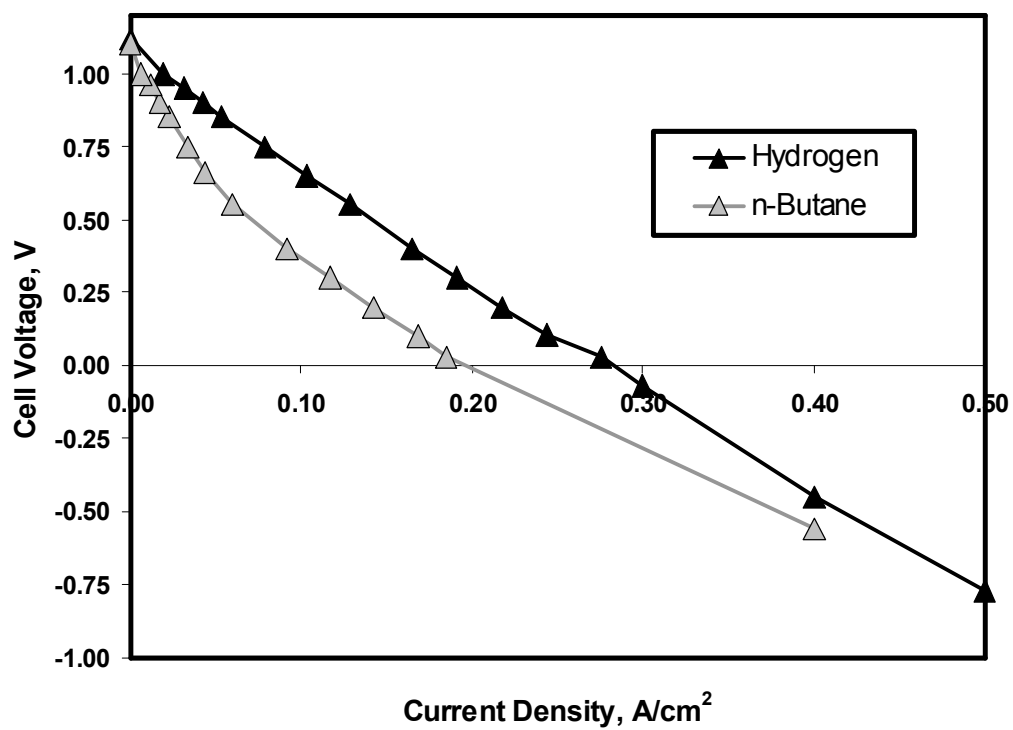
Figure 2(b)
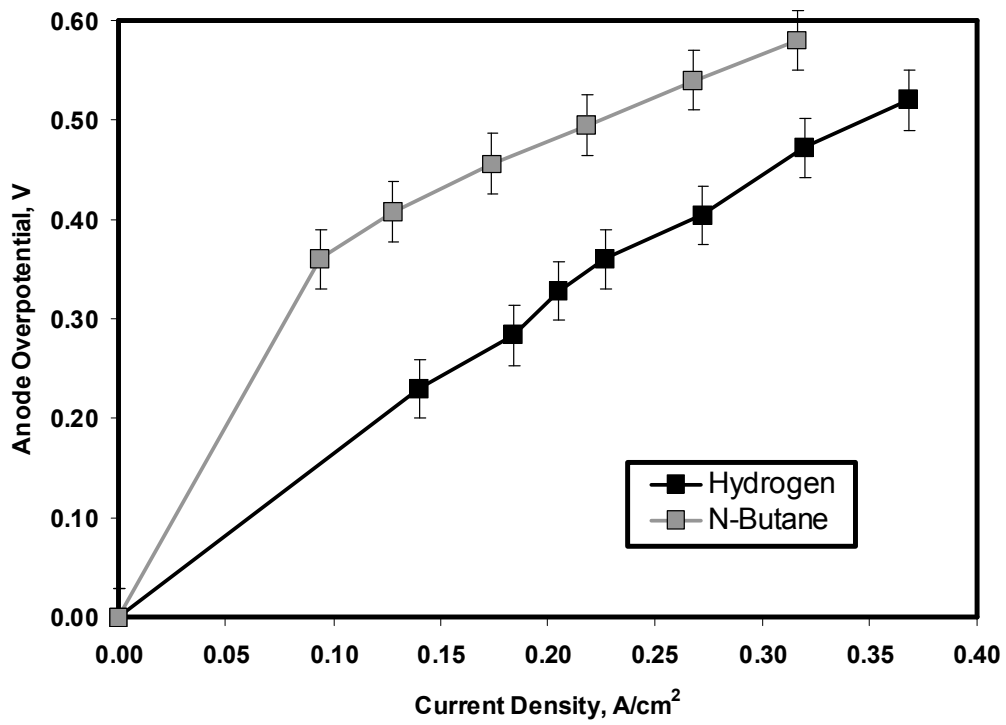
Figure 3(a)
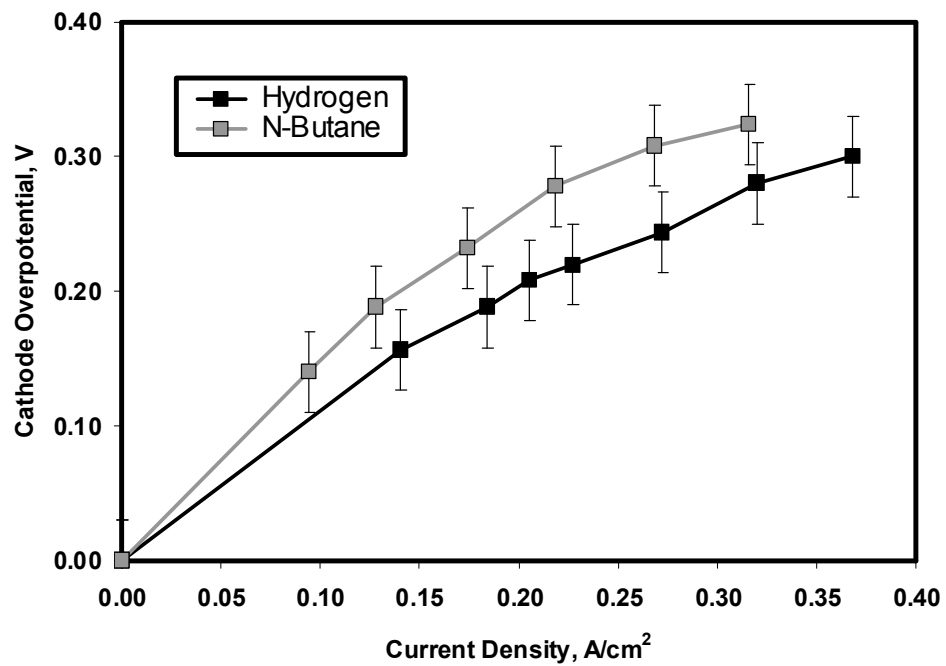
Figure 3(b)
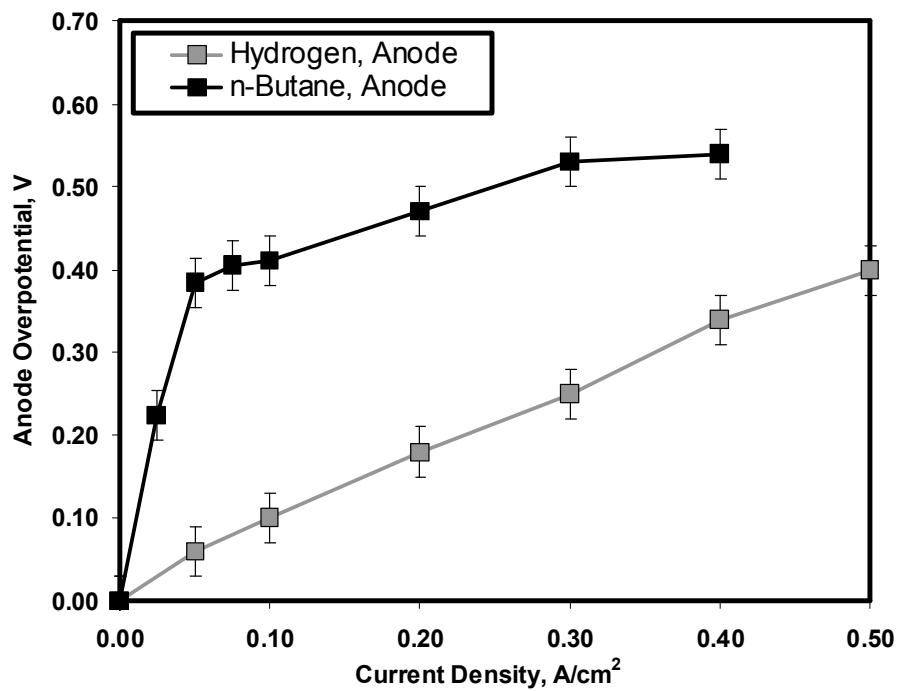
Figure 4(a)
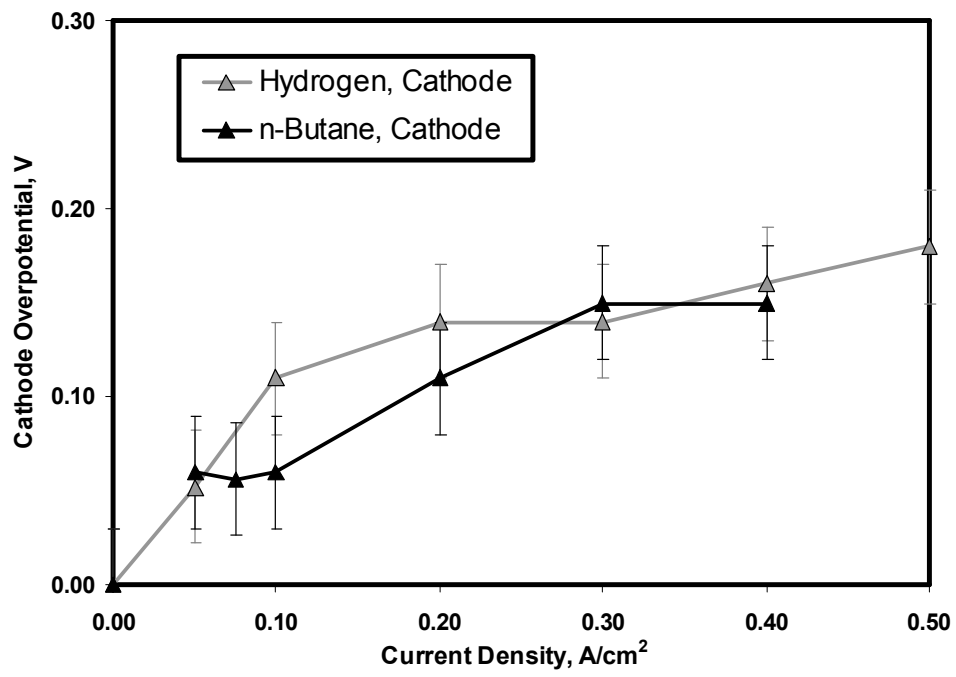
Figure 4 (b)

Figure 5

Figure 6